Signatures of the fast dynamics in glassy polystyrene by multi-frequency, high-field Electron Paramagnetic Resonance of molecular guests

V.Bercu [a,b], M.Martinelli [b], C.A.Massa, [b], L.A.Pardi [b],

D. Leporini [a,c],*

[a]*Dipartimento di Fisica "Enrico Fermi", Università di Pisa, Largo B. Pontecorvo 3, I-56127 Pisa, Italy*

[b]*Istituto per i processi Chimico-Fisici-Consiglio Nazionale delle Ricerche (IPCF-CNR), via G.Moruzzi 1, I-56124 Pisa, Italy*

[c]*INFM-CRS SOFT, Largo B.Pontecorvo 3, I-56127 Pisa, Italy*

Abstract

The reorientation of one small paramagnetic molecule (spin probe) in glassy polystyrene (PS) is studied by high-field Electron Paramagnetic Resonance spectroscopy at three different Larmor frequencies ($95, 190$ and $285\ GHz$). Two different regimes separated by a crossover region are evidenced. Below $180K$ the rotational times are nearly temperature-independent with no apparent distribution. In the temperature range $180 - 220K$ a large increase of the rotational mobility is observed with widening of the distribution of correlation times which exhibits two components: i) a delta-like, temperature-independent component representing the fraction of spin probes w which persist in the low-temperature dynamics; ii) a strongly

temperature-dependent component, to be described by a power-distribution, representing the fraction of spin probes $1 - w$ undergoing activated motion over an exponential distribution of barrier heights $g(E)$. Above $180K$ a steep decrease of w is evidenced. The shape and the width of $g(E)$ do not differ from the reported ones for PS within the errors. The large increase of the rotational mobility of the spin probe at $180K$ is ascribed to the onset of the fast dynamics detected by neutron scattering at $T_f = 175 \pm 25K$.

1 Introduction

Particular interest and a current subject of strong controversy is the so called fast dynamics of glasses, occurring in the time window $1 - 10^2 \, ps$ with several studies carried out mainly by neutron [1–5], Raman scattering [6–9] and high-field Electron Paramagnetic Resonance (HF-EPR) [10,11]. It is observed that on heating in a temperature range below the glass transition temperature T_g the dynamics of glass-forming systems deviates from the harmonic behavior and quasielastic scattering starts to accumulate in the low frequency range of the scattering function $S(Q, \omega)$. Accordingly, the temperature dependence of the atomic mean-squared displacement also starts to deviate from the linear dependence. We will denote by T_f the onset temperature above which the deviation from the harmonic behavior becomes apparent.

* Corresponding author.
  Email address: `dino.leporini@df.unipi.it` (D. Leporini).

The microscopic origin of the fast dynamics is still a question open to a strong controversy. The role of carbon-carbon torsional barriers to drive the fast dynamics of glass-forming polymers was also pointed out [1]. In the particular case of polystyrene (PS) of interest here, T_f was found to be $175 \pm 25K$ [3] and $200K$ [4]. For PS the onset of the fast motion has been ascribed to the change of the *librational* dynamics of the side-chain phenyl ring [3,4] with expected involvement of the main-chain through the connecting bonds [12,13]. According to Nuclear Magnetic Resonance (NMR) the flip motion becomes frozen at about $190K$ [14].

In glasses the dynamics is thermally activated in the substructures of the minima of the energy landscape [15]. Important information is conveyed by the energy barrier distribution $g(E)$ which is only weakly temperature-dependent in the glassy state [16]. For glassy PS this was tested by scaling light scattering data [17]. Buchenau confirmed that conclusion by comparing results from several techniques covering a wide time window from $1Hz$ up to about $100GHz$ [18]. The same result has been reached by HF-EPR [10,11,19].

The shape of the energy-barriers distribution $g(E)$ in glasses has been extensively investigated via experiments [8,10,11,16,17,19–24], theories [25–29] and simulations [30]. Basically, two different distributions are usually recovered, the gaussian distribution [8,16,20,21,24,25,30,31] and the exponential distribution [8,10,11,17,19,22,26–29].

It is interesting to relate $g(E)$ with the density of states, i.e.the distribution of the minima of the energy landscape. On the upper part of the landscape, being explored at high temperatures, the Central Limit theorem suggests that the density is gaussian [30]. At lower temperatures the state point is trapped

3

in the deepest low-energy states which are expected to be exponentially distributed following general arguments [27]. Different models [28] and numerical simulations [29] support the conclusion. In particular, trap models suggest that $g(E)$ has the same shape of the exponential density of states [28] .

If the average trapping time τ before to overcome the barrier of height E at temperature T is governed by the Arrhenius law,

$$\tau = \tau_0 exp(E/kT) \tag{1}$$

k being the Boltzmann's constant, the distribution of barrier heights induces a distribution of trapping times $\rho(\tau)$. The explicit form of $\rho(\tau)$ for an exponential distribution of barrier heights with width $\overline{E}$ is:

$$g(E) = \begin{cases} 0 & \text{if } E < E_{min} \\\\ \frac{1}{\overline{E}} exp(-\frac{E-E_{min}}{\overline{E}}) & \text{if } E \geq E_{min} \end{cases} \tag{2}$$

and $\rho(\tau)$ is expressed by the power-law distribution (PD)

$$\rho_{PD}(\tau) = \begin{cases} 0 & \text{if } \tau < \tau_{PD} \\\\ x\tau_{PD}^x \tau^{-(x+1)} & \text{if } \tau \geq \tau_{PD} \end{cases} \tag{3}$$

with $x = kT/\overline{E}$ and $\tau_{PD} = \tau_0 \, exp(E_{min}/kT)$. Note that the absence of energy barriers below E_{min} does not change the shape of ρ_{PD} and allows for the temperature dependence of τ_{PD}.

If the width of the energy-barriers distribution is vanishingly small, a single

trapping time, i.e. a single correlation time (SCT), is found with:

$$\rho_{SCT}(\tau) = \delta(\tau - \tau_{SCT}) \tag{4}$$

The use of suitable probes to investigate the relaxation in glasses by NMR [14,20,21,23,32], EPR [31,33–35] and Phosphorescence [36] studies is well documented. In particular, during the last few years continuous-wave (CW) and pulsed HF-EPR techniques were developed involving large polarizing magnetic fields, e.g. $B_0 \cong 3T$ corresponding to Larmor frequencies about $95GHz$ (W band), [37,38] or even larger frequencies [19,39,40]. HF-EPR is widely used in polymer science [10,11,19,41–44]. One major feature is the remarkable orientation resolution [44] due to increased magnitude of the anisotropic Zeeman interaction leading to a wider distribution of resonance frequencies [45]. Recently, HF-EPR studies evidenced the exponential distribution of the energy barriers of the deep structure of the energy landscape [19] as well as clear signatures of the onset of fast motion in glassy PS [43,44] in full agreement with neutron [1–5] and Raman scattering [6–9]. These studies were carried out at 190 and 285 GHz. Here, novel results from HF-EPR at $95GHz$ are presented and compared to the previous ones.

2　EPR background

2.1　Lineshape

The EPR signal is detected in paramagnetic systems. Since most polymers are diamagnetic, paramagnetic probe molecules (spin probes) are usually

dissolved in them. The main broadening mechanism of the EPR line shape of the spin probe is determined by the coupling between the reorientation of the latter and the relaxation of the electron magnetization $\mathbf{M}$ via the anisotropy of the Zeeman and the hyperfine magnetic interactions. When the molecule rotates, the coupling gives rise to fluctuating magnetic fields acting on the spin system. The resulting phase shifts and transitions relax the magnetization and broadens the resonance [45]. One important parameter to describe the rotational dynamics of the spin probe is the correlation time τ_l, i.e. the area below the self-correlation function $< Y_{l,0}(t)\, Y_{l,0}(0) >$, $Y_{l,0}$ being the spherical harmonic with rank l .

The occurrence of a static distribution of correlation times in glasses leads to evaluate the EPR line shape $L(B_0)$, which is usually detected by sweeping the static magnetic field B_0 and displaying the first derivative, as a weighted superposition of different contributions:

$$L(B_0) = \int\limits_0^\infty d\tau_2 L(B_0, \tau_2)\, \rho(\tau_2) \tag{5}$$

where $L(B_0, \tau_2)$ is the EPR line shape of the spin probes with correlation time τ_2 and $\rho(\tau_2)$ is the τ_2 distribution. The choice of labeling the different contributions by τ_2 is arbitrary. An efficient numerical method to calculate the HF-EPR line shape is detailed elsewhere [42].

2.2 Model of the rotational motion

One expects that small spin probes undergo jump dynamics in glasses [34]. In the presence of jumps correlations are lost roughly after one single trapping

time, i.e. $\tau_l \cong \tau$. For $l = 2$ a simple rotational jump model yields [34]

$$\tau_2 = \frac{\tau^*}{\left[1 - \frac{\sin\left(\frac{5\phi}{2}\right)}{5\sin\left(\frac{\phi}{2}\right)}\right]} \tag{6}$$

where ϕ and τ^* are the size of the angular jump and the mean residence (trapping) time before a jump takes place, respectively. In the limit $\phi << 1$ eq.6 reduces to $\tau_2 = 1/6D = \tau^*/\phi^2$, where D is the rotational diffusion coefficient, i.e. the isotropic diffusion model. If $\phi \cong 1$, $\tau_2 \cong \tau^*$. Similar conclusions are drawn for arbitrary l values. The above discussion suggests that in the presence of jump dynamics the distribution of the rotational correlation times τ_l and the distribution of trapping times τ of the spin probe do not differ too much. Henceforth, to emphasize that viewpoint, τ_2 will be denoted as τ.

The identification of the rotational correlation time with the waiting time before one activated jump takes place, is questionable when the latter becomes extremely rare. In fact, if energy barriers are too high, entropic-like, alternative pathways may become competitive to cancel the orientation correlations. A simple account of that is provided by the truncation of $\rho(\tau)$ in eq.5 beyond a certain τ_{max} to give an effective distribution

$$\rho_T(\tau) = H(\tau_{max} - \tau)\rho(\tau) + w\delta(\tau - \tau_{max}) \tag{7}$$

where $\delta(x)$ is the Dirac delta, $H(x) = 1$ for $x > 0$ and zero otherwise and

$$w = \int_{\tau_{max}}^{\infty} d\tau \, \rho(\tau) \tag{8}$$

The weight w is the fraction of *trapped* molecules, i.e. the ones losing the rotational correlations by undergoing not-activated motion. Henceforth, ρ_{TPD} will

denote ρ_T in the particular case $\rho = \rho_{PD}$, eq.3 with $\tau_{PD} < \tau_{max}$. Representative plots of the bimodal distribution ρ_{TPD} are shown in fig.1.

2.3 Adjustable parameters

The data analysis fits the experimental HF-EPR lineshapes collected at different temperatures and to the operating frequency of $95GHz$ with the theoretical prediction as expressed via eq.5 and the proper distribution function ρ_T, eq.7. It is worthwhile to state explicitely the number of adjustable parameters. They are divided in two sets:

i) the parameters which are temperature- and frequency- independent. The set includes the six magnetic parameters of the spin probe (the principal components of the g and hyperfine tensors) and the jump angle ϕ;

ii) the parameters which are temperature-dependent and almost frequency-independent. The set includes the width of the energy-barrier distribution, e.g. $\overline{E}$ for the exponential distribution, eq.2, and the characteristic time scales of ρ_T, eq.7. In the case $\rho_T = \rho_{TPD}$, they are the shortest and the longest correlation time τ_{PD} and τ_{max} respectively. Having set the former time scales the weight w is not adjustable. In the simplest case of no distribution of correlation times (eq.4) τ_{SCT} only is adjusted.

The fit of the HF-EPR lineshapes by eq.5 provides the best-fit values of the adjustable parameters and their errors which follow by suitable χ^2 evaluation.

8

3   Experimental details

Atactic PS was obtained from Aldrich and used as received. The weight-average molecular weight is M_w=230 kg mol^{-1}, polydispersity $M_w/M_n = 1.64$ and T$_g$=367 K. The free radical used as spin probe was 2,2,6,6-tetramethyl-1-piperidinyloxy (TEMPO) from Aldrich. TEMPO has one unpaired electron spin S=1/2 subject to hyperfine interaction with the nitrogen nucleus with spin I=1. The chemical structures of PS and TEMPO are shown in fig.2.

Notice that TEMPO and the phenyl group of PS have similar shape. TEMPO is stiff with almost spherical shape [35]. It has an average van der Waals radius $r_{TEMPO} = 3.3 \pm 0.2 \mathring{A}$ and may be sketched as an oblate ellipsoid with semiaxes $r_{\parallel} \sim 2.7 \mathring{A}$ and $r_{\perp} \sim 3.7 \mathring{A}$. The preparation of the sample is described elsewhere [11]. The spin probe was less then 0.08% in weight, thus resulting in a extremely limited influence on PS. The EPR experiments at $95 GHz$ were carried out on the ultrawide-band EPR spectrometer which is detailed elsewhere [46]. Magnetic parameters of TEMPO are drawn from our previous studies on TEMPO in PS [11].

4   Results

Fig. 3 shows the lineshape at $95 GHz$ of TEMPO in PS at $50K$. It is seen that the lineshape is well fitted by a *single* correlation time (SCT model, eq.4, two adjustable parameters, τ_{SCT}, ϕ). The small discrepancy between the simulation and the peak at low magnetic field was already noted [38]. At such very slow reorientation rates the lineshape is weakly sensitive to the jump size. In fact, the quality of the fit does not change if the jump angle ϕ spans the

range $20° - 60°$.

Fig. 4 shows the lineshape at $95GHz$ of TEMPO in PS at $T = 180K$. Again, the SCT model provides good fits even if discrepancies are larger than at $50K$. The faster rotational rate allows for better definition on the jump angle ϕ whose best-fit value is in the range $20° - 35°$.

Fig. 5 shows the lineshape of TEMPO in PS at $T = 200K$. Here, the best-fit curve by using the SCT model deviates from the experiment. Better agreement is provided by considering the truncated power distribution of correlation times ρ_{TPD} (eq.7 with $\rho = \rho_{PD}$, eq.3). Following refs.[10,11], τ_{max}, the rotational correlation time of trapped TEMPO (Sec.2.2) is set equal to τ_{SCT} at $180K$, i.e. the rotational dynamics of TEMPO for $T \leq 180K$ is assumed to be non-activated (in fact τ_{SCT} between $50K$ and $180K$ is found almost temperature-independent, see figs.3,4). That constraint was kept for all the temperatures $T \geq 200K$. Due to this strategy, $\rho_{TPD}(\tau)$ adds only *one* adjustable parameter to the one of the elementary SCT model, eq.4.

At higher temperatures the agreement of the TPD model with the experiment becomes much more pronounced than in Fig.5. This may be understood by considering Fig.6. It shows that, on increasing the temperature, the fraction of trapped TEMPO molecules w decreases markedly, making the differences between TPD and PD models immaterial. The excellent agreement of the PD model with the experimental findings on the reorientation of TEMPO in PS at $240K$ and $270K$ was reported elsewhere [10,11,19].

Fig.6 also presents the temperature dependence of the width of the energy-barrier distribution $\overline{E} = kT/x$ as drawn by best-fit procedure of the HF-EPR

lineshapes at $95, 190$ and $285 GHz$ in terms of the TPD model. To get that results, the parameters x, and τ_{PD} of eq.3 only were adjusted with constant jump angle $\phi = 20°$. The lowest temperature of the plot is $200K$, below which TEMPO is fully trapped ($w \cong 1$, fig.6) and then unable to probe the energy-barrier distribution.

Fig.7 presents the overall temperature dependence of the characteristic times describing the reorientation of TEMPO according to the SCT (eq.4, τ_{SCT}) , PD (eq.3, τ_{PD}) and TPD (eq.7 with $\rho = \rho_{PD}$, τ_{PD} and τ_{max}) models.

5   Discussion

It is interesting to compare the exponential energy-barrier distribution which is experienced by TEMPO, $g(E)$, and $g_{PS}(E)$, i.e. the exponential distribution of barrier-heights of PS which was evidenced by internal friction [22], Raman [8] and light scattering [17]. The measured widths were $\overline{E}_{IF}/k = 760 \pm 40K$, $\overline{E}_{Raman}/k = 530 \pm 60K$ and $\overline{E}_{LS}/k = 530 \pm 40K$, respectively. Fig.6 shows that the distribution of energy barriers $g(E)$ probed by TEMPO has not only the same exponential shape of the PS one, but it exhibits also comparable width. In particular, the constancy of $\overline{E}$ for TEMPO at low temperatures is consistent with the conclusion that the latter probes the barrier-height distribution of glassy PS which is expectedly temperature-independent [16]. The apparent decrease of $\overline{E}$ at the highest temperature is, most probably, not due to PS which is still well below T_g but to faster reorientation of TEMPO leading to a decoupling from PS dynamics. The increase of the width of the exponential distribution $g(E)$, $\overline{E}$, with the HF-EPR frequency is under current investigation and will be discussed elsewhere. Notably, the frequency-dependence of $\overline{E}$

11

decreases at the highest temperature under investigation, i.e. $270K$.

Fig.7 shows the temperature dependence of the characteristic times of TEMPO in PS. On heating, after a flat region between $50 - 180K$ where TEMPO exhibits a single correlation time τ_{SCT}, between $180 - 220K$ a second component of the distribution of correlation times arises, being described by a truncated power distribution of correlation times whose shortest timescale τ_{PD} drops of a factor of about 80. The increase of the rotational mobility parallels the strong decrease of the fraction of trapped TEMPO molecules w, fig.6. The changes of the bimodal distribution of correlation times by decreasing w is pictured by fig.1. Interestingly, similar effects on guest molecules were reported. NMR showed that toluene (similar in shape to TEMPO, see fig.4) in glassy PS exhibits both frozen and mobile components, the latter arising at about $170 - 180K$ [14,32]. Moreover, it was noted by EPR that oriented spin probes in PS lose their alignment above $\cong 200K$ [33]. It is worthwhile to point out that the change of the rotational dynamics of TEMPO in PS around $200K$ cannot be ascribed in an obvious way to changes in the free-volume where TEMPO is accomodated, as in other cases [35]. In fact, the study of the unoccupied volume of PS by the positron annihilation technique showed that the free-volume size increases smoothly with trivial linear temperature-dependence in the range $30 - 260K$ [47].

We intepret the increased rotational mobility of TEMPO above $180K$ as a signature of the onset of the fast dynamics of PS which, according to neutron scattering studies is located at $T_f = 175 \pm 25K$ [3,4]. In fact, our results suggest the following scenario. Below $180K$ TEMPO molecules are unable to hop over barriers. The orientation correlations are lost by non-activated entropic-like processes with negligible distribution of the characteristic timescales. Above

12

that temperature the onset of fast PS dynamics, which is well coupled to the rotational timescales of TEMPO, facilitate the crossover of the barriers which is successfully accomplished by a fraction $(1-w)$ of TEMPO molecules. Jumping over the barriers allows TEMPO to probe the exponential distribution of PS barrier-heights. As a consequence, a distribution of correlation times arises.

6   Conclusions

The reorientation of the spin probe TEMPO in PS has been studied by high-field Electron Paramagnetic Resonance spectroscopy at three different Larmor frequencies ($95, 190$ and $285\ GHz$). Two different regimes separated by a crossover region are evidenced. Below $180K$ the rotational times are nearly temperature-independent with no apparent distribution. In the temperature range $180 - 220K$ a large increase of the rotational mobility is observed with widening of the distribution of correlation times which exhibits two components: i) a delta-like, temperature-independent component representing the fraction of spin probes w which persist in the low-temperature dynamics; ii) a strongly temperature-dependent component, representing the fraction of spin probes $1 - w$ undergoing activated motion over an exponential distribution of barrier heights $g(E)$. Above $180K$ a steep decrease of w is evidenced. The shape and the width of $g(E)$ do not differ from the reported ones for PS within the errors. The increase of the rotational mobility of the spin probe at $180K$ is considered as signature of the onset of the fast dynamics detected by neutron scattering at $T_f = 175 \pm 25K$ being ascribed either to the change of the *librational* dynamics of the side-chain phenyl ring [3,4] or the carbon-carbon torsional barriers [1]. Additional work is needed to discriminate between these

two views.

Acknowledgements

J.Colmenero and A.P.Sokolov are gratefully acknowledged for helpful discussions.

References

[1] J.Colmenero, A.Arbe, Phys.Rev.B 57 (1998) 13508.

[2] T.Kanaya, K.Kaji, Adv.Polym.Sci. 154 (2001) 87.

[3] B. Frick, U. Buchenau, and D. Richter, Colloid Polym. Sci. 273 (1995) 413.

[4] T.Kanaya, T.Kawaguchi,K.Kaji, J.Chem.Phys. 104 (1996) 3841.

[5] B.Frick, D. Richter, Phys.Rev.B 47 (1993) 14795.

[6] Y.Ding, V.N.Novikov, A.P.Sokolov, A.Cailliaux, C.Dalle-Ferrier, C.Alba-Simionesco, B.Frick, Macromolecules 37 (2004) 9264.

[7] V.N.Novikov, A.P.Sokolov, B.Strube, N.V.Surovtsev, E.Duval, A.Mermet, J.Chem.Phys. 107 (1997) 1057.

[8] A.P.Sokolov, V.N.Novikov, B.Strube, Europhys.Lett. 38 (1997) 49.

[9] A.P.Sokolov, U. Buchenau, W.Steffen, B.Frick, A.Wischnewski, Phys.Rev.B 52 (1995) R9815.

[10] V.Bercu, M.Martinelli, C.A.Massa, L.A.Pardi, D. Leporini, Europhys. Letters,72 (2005) 590.

[11] V.Bercu, M.Martinelli, C.A.Massa, L.A.Pardi, D. Leporini, J.Chem.Phys., 123 (2005) 174906. .

[12] J.Schaefer, M.D.Sefcik,E.O.Stejskal,R.A.McKay, Macromolecules 17 (1984) 1107.

[13] R.Khare, M.E.Paulaitis, Macromolecules 28 (1995) 4495.

[14] H.Sillescu, Makromol. Chem., Macromol. Symp. 1 (1986) 39.

[15] C.A. Angell, Nature 393 (1998) 521.

[16] L.Wu, S.R.Nagel, Phys.Rev.B 46 (1992) 11198.

[17] N.V.Surovtsev, J.A.H.Wiedersich, V.N.Novikov, E.Rössler, A.P.Sokolov, Phys.Rev.B 58 (1998) 14888.

[18] U.Buchenau, Phys.Rev.B 63 (2001) 104203.

[19] V Bercu, M Martinelli, C AMassa, L A Pardi, D.Leporini, J. Phys.: Condens. Matter 16 (2004) L479.

[20] R. Böhmer , G.Diezemann , G.Hinze , E.Rössler , Prog.Nucl.Mag.Reson. 39 (2001) 191.

[21] F.Qi, R.Böhmer, H.Sillescu, Phys.Chem.Chem.Phis. 3 (2001) 4022.

[22] K.A.Topp, D.G.Cahill, Z.Phys.B 101 (1996) 235.

[23] E.Rössler, M.Taupitz, K.Börner, M.Schulz, H.M.Vieth, J.Chem.Phys. 92(1990) 5847.

[24] M.Vogel, E.Rössler, J.Chem.Phys. 114 (2001) 5802.

[25] H.Bässler, Phys.Rev.Lett. 58 (1987) 767.

[26] T.Odagaki, Phys.Rev.Lett. 75 (1995) 3701.

[27] J -P.Bouchaud, M.Mezard, J.Phys.A: Math.Gen. 30 (1997) 7997.

[28] B.Rinn, P.Maass, J -P.Bouchaud, Phys.Rev.B 64 (2001) 104417.

[29] J.C.Schön, P.Sibani, Europhys.Lett. 49 (2000) 196.

[30] R.A.Denny, D.R.Reichman, J -P Bouchaud, Phys.Rev.Lett. 90 (2003) 025503.

[31] M.Faetti, M.Giordano, D.Leporini, L.Pardi, Macromolecules 32 (1999) 1876 .

[32] E.Rössler, H.Sillescu, H.W.Spiess, Polymer 26(1985) 203.

[33] A.Kh.Vorobiev, V.S.Gurman, T.Klimenko, Phys.Chem.Chem.Phys. 2 (2000) 379.

[34] L.Andreozzi, F.Cianflone, C.Donati, D.Leporini, J.Phys.: Condens.Matter 8 (1996) 3795.

[35] A.Barbieri, G.Gorini, D.Leporini, Phys. Rev. E 69 (2004) 061509.

[36] M.Christoff, T.D.Z.Atvars, Macromolecules 32 (1999) 6093.

[37] M.A.Ondar, O.Y.Grinberg, L.G.Oranskii, V.I.Kurochkin, Y.L.Lebedev, J. Struct. Chem. 22 (1981) 626.

[38] D.E.Budil, K.A.Earle, J.H.Freed, J. Phys. Chem. 97 (1993) 1294.

[39] T.N. Makarov, A.N. Savitsky, K.Mobius, D.Beckert, H.Paul, J.Phys,Chem. A 109 (2005) 2254.

[40] H.Blok, J.A.J.M.Disselhorst, S.B.Orlinskii, J.Schmidt, J.Mag.Reson. 166 (2004) 92.

[41] J.Pilar, J.Labsky, A.Marek, D.E.Budil, K.A.Earle, J.H.Freed, Macromolecules 32 (2000) 4438.

[42] D.Leporini, X.X.Zhu, M.Krause, G.Jeschke, H.W.Spiess, Macromolecules 35 (2002) 3977.

[43] D.Leporini, V.Schädler, U.Wiesner, H.W.Spiess, G.Jeschke, J. of Non-Crystalline Solids 307?310 (2002) 510.

[44] D.Leporini, V.Schädler, U.Wiesner, H.W.Spiess, G.Jeschke, J.Chem.Phys. 119 (2003) 11829.

[45] L.J. Berliner, Spin labeling: Theory and Applications, Academic, New York, 1976); L.J.Berliner and J. Reuben, Biological magnetic resonance, Plenum, New York, Vol 8, 1989.

[46] G.Annino, M.Cassettari, M.Fittipaldi, L.Lenci, I.Longo, M.Martinelli, C.A.Massa and L.A.Pardi, Appl.Magn.Reson. 19 (2000) 495.

[47] A. Uedono, T. Kawano, S. Tanigawa, M. Ban, M. Kyoto, and T. Uozumi, J. Polym. Sci., Part B: Polym. Phys. 34 (1996) 2145.

Figure captions

Fig. 1. Schematic view of the bimodal distribution of correlation times ρ_{TPD} (eq.7 with $\rho = \rho_{PD}$) for different values of the trapped fraction w. $x = 0.8$, τ_{PD} denotes the shortest correlation time. The delta function is replaced by a narrow gaussian with width 0.01.

Fig. 2. Chemical structures of PS and the spin probe TEMPO.

Fig. 3. The line shape at $95GHz$ of TEMPO in PS at $50K$. The superimposed dotted line is the best fit according to the SCT model, eq.4, with $\tau_{SCT} = 29 \pm 3ns$. Jump angle $\phi = 60°$. Nearly identical agreement is obtained by decreasing the jump angle down to $\phi = 20°$ with $\tau_{SCT} = 85 \pm 9ns$. The theoretical lineshape is convoluted by a Gaussian with width $0.15mT$ to account for the inhomogeneous broadening. The same convolution is understood in Figs.4 and 5.

Fig. 4. The lineshape at $95GHz$ of TEMPO in PS at $180K$. The superimposed dotted line is the best fit according to the SCT model with jump angle $\phi = 35°$ and $\tau_{SCT} = 30 \pm 3ns$. Both the quality of the fit and the best-fit value of τ_{SCT} are unchanged within the errors if one sets the jump angle in the range $20° \leq \phi \leq 35°$.

Fig. 5. The EPR line shape at T=200K and frequency $95GHz$. The dashed line is the best fit by using the TPD model (eq.7 with $\rho = \rho_{PD}$, eq.3) with $x = 0.4 \pm 0.04$, $\tau_{PD} = 3 \pm 0.3ns$. The dotted line is the best fit by using the SCT model with $\tau_{SCT} = 17 \pm 2ns$ and the jump angle $\phi = 20°$. The TPD model has only *one* more adjustable parameter with respet to SCT one.

Fig. 6. Temperature dependence of the fraction of trapped TEMPO molecules, eq.8, as measured at $95GHz$ (present work), 190 and $285GHz$ [10,11]. Inset: temperature dependence of the width $\overline{E}$ of the exponential energy-barrier distribution, as detected by the EPR at $95GHz$, 190 and $285GHz$. Previous measurements by internal friction [22], Raman [8] and light scattering [17] yield $\overline{E}_{IF}/k = 760 \pm 40K$,$\overline{E}_{Raman}/k = 530 \pm 60K$ and $\overline{E}_{LS}/k = 530 \pm 40K$, respectively. Dotted lines are guides for the eye.

Fig. 7. Temperature dependence of the characteristic times of the SCT, PD and TPD distributions as drawn from the best fit of the lineshapes at $95GHz$ (present work), 190 and $285GHz$ [10,11].. The error bars at $50K$ and $180K$ account for the uncertainty on the best-fit value of the jump angle which is in the range $20° \leq \phi \leq 60°$, $20° \leq \phi \leq 35°$, respectively . Dotted lines are guides for the eye.

FIGURE 1

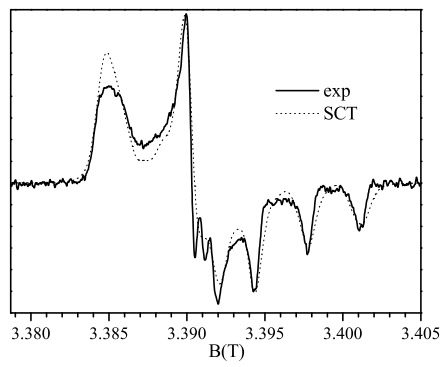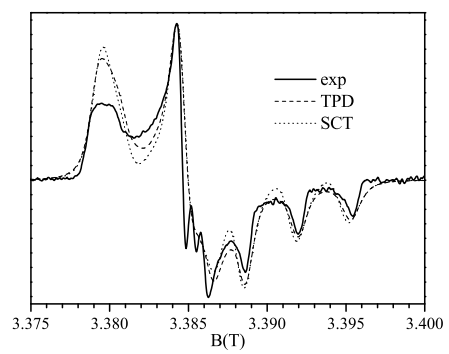PS   TEMPO
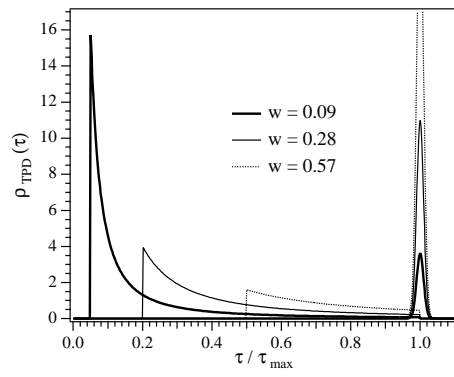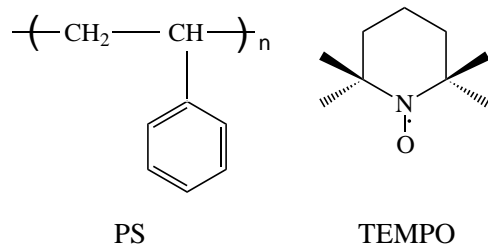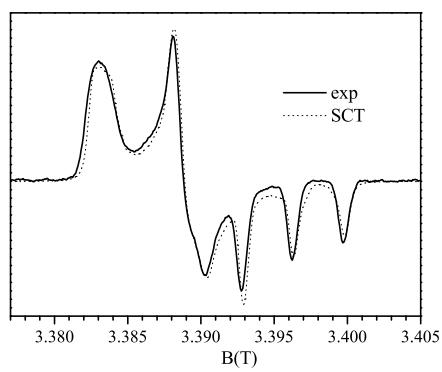
FIGURE 2

FIGURE 3

FIGURE 4

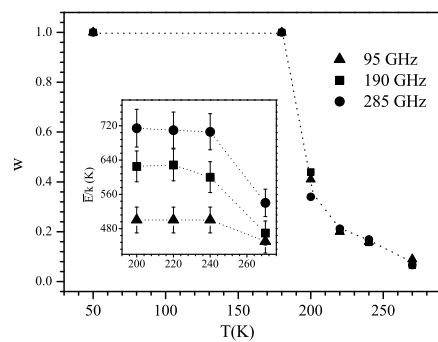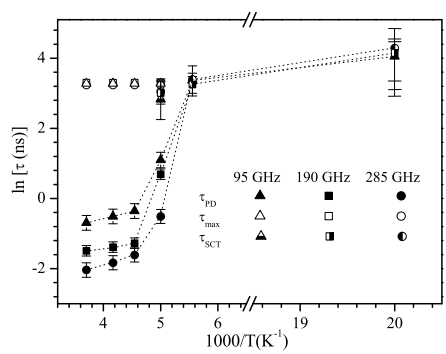**FIGURE 5**

FIGURE 6

FIGURE 7